fermentation

MDPI

Article

Bioethanol Production via Herbaceous and Agricultural Biomass Gasification Integrated with Syngas Fermentation

Sahar Safarian [1,2,*], Runar Unnthorsson [1] and Christiaan Richter [1]

[1] Faculty of Industrial Engineering, Mechanical Engineering and Computer Science, University of Iceland, Hjardarhagi 6, 107 Reykjavik, Iceland; runson@hi.is (R.U.); cpr@hi.is (C.R.)
[2] Department of Technology Management and Economics, Division of Environmental Systems Analysis, Chalmers University of Technology, 412 96 Gothenburg, Sweden
* Correspondence: sas79@hi.is

Abstract: In this paper, a simulation model based on the non-stoichiometric equilibrium method via ASPEN Plus was established to analyze the gasification performance of 20 herbaceous and agricultural biomasses (H&ABs) linked with syngas fermentation and product purification units for ethanol production. The established simulation model does not consider the gasification system as a black box; it focuses the important processes in gasification such as drying, pyrolysis, gasification, and connection with bioethanol production plants. The results for the 20 H&AB options suggest that the specific mass flow rate of bioethanol from 1 kg of biomass input to the unit is in the range of 99–250 g/kg, and between them, the system fed by hazelnut shell biomass remarkably outranked other alternatives by 241 g/kg production due to the high beneficial results gained from the performance analysis. Additionally, a sensitivity analysis was performed by changing operating conditions such as gasification temperature and air-to-fuel ratio. The modeling results are given and discussed. The established model could be a useful approach to evaluate the impacts of a huge numbers of biomasses and operating parameters on bioethanol output.

Keywords: bioethanol production; gasification; herbaceous and agricultural biomass; syngas fermentation; simulation

Citation: Safarian, S.; Unnthorsson, R.; Richter, C. Bioethanol Production via Herbaceous and Agricultural Biomass Gasification Integrated with Syngas Fermentation. *Fermentation* **2021**, *7*, 139. https://doi.org/10.3390/fermentation7030139

Academic Editor: Christian Kennes

Received: 30 June 2021
Accepted: 29 July 2021
Published: 31 July 2021

1. Introduction

Consuming and burning fossil fuels for energy production has negatively affected modern health, society, and environment, which has led to increases of the application of renewable energy sources and alternative technologies to produce energy, heat, and power [1–3]. In the last few decades, interest in biomass has sharply increased because of the increased attention to sustainable energies [4–7]. Herbaceous and agricultural biomasses (H&ABs) are currently the most critical and abundant sources of renewable energy in the world that can be used for energy generation. In fact, herbaceous crops have the highest ranking for bioenergy production due to their high biomass yield, high net energy gain, and biomass quality that make them suitable for both biochemical and thermochemical conversion [8]. H&ABs come from plants that have non-woody stems and that die at the end of their growing seasons. This biomass includes most agricultural crops, grasses, and straws. Herbaceous biomass has a higher nutrient content and a lower lignin content than wood. Generally, the lignin and cellulose contents in H&ABs are in the range of 18–35 wt% and 65–75 wt%, respectively [9].

Bioethanol is one of the most promising biofuels that can be consumed in cars with detached engines or as an additive in fuel blending up to 30% without any amendments to an engine [10–12]. Currently, 11% of worldwide energy consumption is satisfied by using biomass, and most of this value comes from bioethanol production. This bioethanol is mainly obtained via sugar- and starch-based materials like sugarcane and grains. However, these kids of materials must compete with food security and extend deforestation.

The third group is lignocellulosic materials, which is the most sustainable material for bioethanol production with no negative effects on food security and competitiveness with agricultural crops [13–15]. These types of feedstocks can be transformed to ethanol by applying biochemical or thermochemical conversion processes. Biochemical conversion involves hydrolysis and fermentation, while thermochemical conversion involves gasification and syngas fermentation [16,17]. Syngas fermentation is performed with no need for expensive pretreatment processes or enzymes, as well as at intermediate temperatures and pressures [18]. Furthermore, the environmental effects rated to inlets are neglected in thermochemical conversion processes. However, biochemical conversion does not require sulfuric acid, lime, and nutrients, which greatly contribute to life cycle fossil fuel consumption, GHG emissions, and water use [16,19,20]. Therefore, employing H&AB gasification systems linked with syngas fermentation could be a feasible and sustainable option for bioethanol production.

Syngas fermentation into ethanol and other bioproducts has been considered to be more attractive than the biochemical approach due to several inherent merits such as the utilization of the whole biomass including lignin regardless of the biomass quality; the elimination of complex pretreatment steps, and costly enzymes; the aseptic operation of syngas fermentation due to the generation of syngas at higher temperatures and bioreactor operation at ambient conditions. This process has been studied by several researchers. Phillips et al. [21] proposed a conceptual model for the description of syngas fermentation through a review of the feedstocks, syngas production, metabolic pathways, bioreactor design, mass transfer, thermodynamics, electrochemistry, and microbial kinetics of the syngas fermentation process. Medeiros et al. [22] developed a dynamic model for the production of ethanol via syngas fermentation in a CSTR, and unknown kinetic parameters were estimated with literature data by employing different gas flow rate, dilution rate, syngas composition, and medium composition conditions. The modeling framework was then used to evaluate the effects of different input variables on the outcomes of ethanol productivity and gas conversion, and it was observed that cell recycle rate, gas flow rate, and H_2 content had clear positive effects on productivity while the dilution rate gave different maximums depending on the other variables. Broadly speaking, syngas fermentation an option for future, sustainable biobased economies due to its potential as an intermediate step in the conversion of waste biomass to ethanol and other biofuels, and its integration with gasification makes it an efficient and competitive route for the valorization of various biowastes, especially if system engineering principles are employed to target process optimization [22–24]. However, the authors are not aware of any research into the simulation modeling of integrated downdraft biomass gasification with syngas fermentation for ethanol production that has evaluated the effects of herbaceous and agricultural biomass and different process parameters on system performance.

The primary goal of this paper was to establish a simulation model relying on the non-stoichiometric equilibrium method via ASPEN Plus for the performance evaluation of 20 H&ABs in downdraft gasification linked with syngas fermentation and product recovery units. The aim was to rank the most efficient H&AB for bioethanol production. Then, a sensitivity analysis of the effect of the temperature and air-to-fuel ratio (ARF) operating conditions to reveal the optimal states of the system to find the maximum possible bioethanol output.

2. Materials and Methods

A simulation model based on the non-stoichiometric equilibrium method was established for bioethanol production by applying ASPEN Plus software. The established model relied on H&AB gasification linked with syngas fermentation and product recovery units for bioethanol production. The Penge Robinson and Boston–Mathias alpha functions have been used for state equations to compute the physical properties of the conventional materials in the system [25,26]. The NRTL model was also considered for the thermodynamic package of phase equilibrium among various components in a mixture containing a water–

ethanol azeotrope [17]. Here, HCOALGEN and DCOALIGT modeling approaches were selected for the enthalpy and density modeling of biomass and ash as non-conventional materials in such a system. The MCINCPSD stream used here includes 3 streams of the MIXED, CIPSD, and NCPSD classes while also showing the structures of biomass and ash that are not available in Aspen Plus materials database [27,28]. The flow chart of the gasification plant simulated via ASPEN Plus is presented in Figure 1.

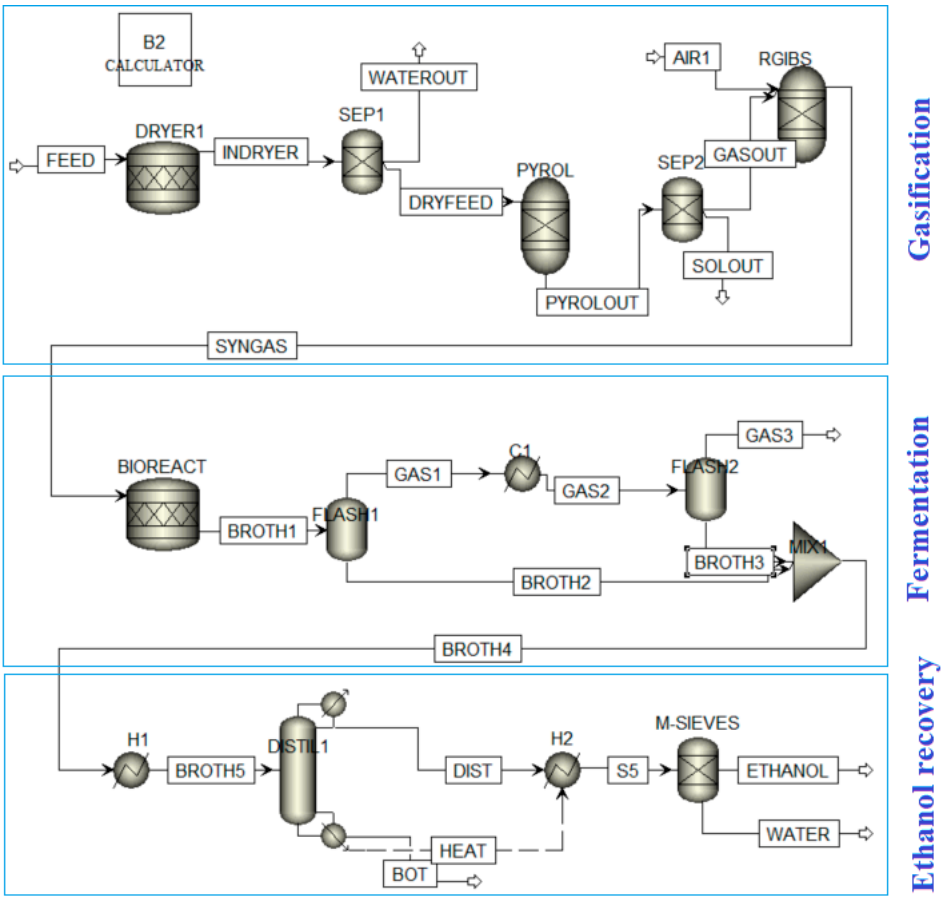

Figure 1. Aspen Plus flow chart of the system.

The BIOMASS stream is represented as a nonconventional stream, and it was made by defining the specific elemental and gross compositions of feedstock attained by proximate and elemental analyses. In this paper, 20 biomass feedstocks from the H&AB group were used as input to be fed to the gasifier. The results of proximate and elemental analyses of the considered biomasses are summarized in Table 1 [29–44].

The first step in the gasification process was drying, which had to happen at a temperature of 150 °C to reach a moisture reduction of less than 5 wt.% of the original sample. This stage was performed by the RSTOIC module as the stoichiometric reactor in the Aspen Plus. This unit was utilized to direct the chemical reactions with known stoichiometry [45]. After the drying step, the RYIELD module (the yield reactor) was modeled to show the performance of feed pyrolysis. In this stage, the biomass was converted to volatile materials (VMs) and char. VMs include carbon, hydrogen, oxygen, and nitrogen, and char could also be converted to ash and carbon by specifying the product distribution based on the proximate and ultimate analysis of the biomass. Next, the RGibbs module was used to model biomass gasification. The decomposed feed and air were entered into the RGibbs reactor, where partial oxidation and gasification reactions were performed. This reactor computed the mole and mass fractions of components within the syngas product by minimizing the Gibbs free energy and assumed complete chemical equilibrium [46–48].

Table 1. Elemental and proximate analyses of 29 herbaceous and agricultural biomasses. M: moisture; VM: volatile materials; FC: fixed carbon; A: ash; C: carbon; O: oxygen; H: hydrogen; N: nitrogen; S: sulphur.

		Proximate Analysis (wt%)				Elemental Analysis (wt%—Dry Basis)				
		M	**VM**	**FC**	**A**	**C**	**O**	**H**	**N**	**S**
1	Bamboo whole	13	81.6	17.5	0.9	51.53	42.1	5.054	0.396	0
2	Kenaf grass	7.5	79.4	17	3.6	46.66	42.9	5.784	0.964	0.0964
3	Miscanthus grass	11.4	81.2	15.8	3	47.72	42.9	5.82	0.388	0.194
4	Sweet sorghum grass	7	77.2	18.1	4.7	47.36	41.6	5.813	0.381	0.0953
5	Switchgrass	11.9	80.4	14.5	5.1	47.17	41.2	5.789	0.664	0.0949
6	Barley straw	11.5	76.2	18.5	5.3	46.78	41.3	5.871	0.663	0.0947
7	Corn straw	7.4	73.1	19.2	7.7	44.95	40.7	5.907	0.646	0.0923
8	Oat straw	8.2	80.5	13.6	5.9	45.92	42	5.646	0.471	0.0941
9	Rape straw	8.7	77.4	17.9	4.7	46.22	42.4	6.099	0.477	0.0953
10	Rice straw	7.6	64.3	15.6	20.1	40.03	34.4	4.554	0.799	0.1598
11	Almond shells	7.2	74.9	21.8	3.3	48.64	41.1	5.995	0.967	0
12	Coconut shells	4.4	73.8	23	3.2	49.46	41.7	5.421	0.097	0.0968
13	Coffee husks	10.8	76.5	20.7	2.8	44.13	46.9	4.763	1.069	0.2916
14	Rice husks	10.6	62.8	19.2	18	40.43	35.8	5.002	0.656	0.082
15	Soya husks	6.3	74.3	20.3	5.4	42.95	44.4	6.338	0.851	0.0946
16	Sugar cane bagasse	10.4	85.5	12.4	2.1	48.75	43	5.874	0.196	0.0979
17	Walnut hulls and blows	47.9	79.6	17.5	2.9	53.5	35.4	6.506	1.554	0.0971
18	Pepper residue	9.7	64.8	27	8.2	41.95	43.2	2.938	3.121	0.5508
19	Grape marc	10	65.8	26.4	7.8	49.79	34.5	5.624	2.213	0.0922
20	Hazelnut shells	7.2	77.1	21.4	1.5	50.73	41	5.418	1.379	0

Next, the produced syngas entered the fermentation process, where it was converted into ethanol and acetic acid in the fermenter via an acetogenic microorganism such as *Clostridium ljungdahlii*. The fermentation section was modeled by applying the BIOREACT module as a stoichiometric reactor in Aspen Plus operated at atmospheric pressure and 38 °C. This temperature was considered because it is the optimal temperature for growth of most ethanol-producing acetogenic microorganisms. The modeling of the bioreactor was based on the research carried out by Ray and Ramachandran [49]. In the bioreactor, 70% and 5% of CO were converted to ethanol and acetic acid, respectively, while 50% of H_2 and 2% were converted to ethanol and acetic acid, respectively (according to the following reactions):

$$4CO + 2H_2O \rightarrow CH_3COOH + 2CO_2 \quad (1)$$

$$2CO_2 + 4H_2 \rightarrow CH_3COOH + 2H_2O \quad (2)$$

$$6CO + 3H_2O \rightarrow C_2H_5OH + 4CO_2 \quad (3)$$

$$2CO_2 + 6H_2 \rightarrow C_2H_5OH + 3H_2O \quad (4)$$

The bioreactor containing cells of the acetogenic bacteria (cell broth or beer) was a vessel designed to promote the transfer of CO and H_2 into the cells in the beer. CO and H_2 were transformed to ethanol via reactions mediated by enzymes inside the cells. The product stream was a combination of liquid and gas that had to be separated. A series of cooler and flash units was used to model this separation, thus minimizing the ethanol lost in the exhaust gas (GAS3).

In order to use the bioethanol product as a biofuel, a high purity product is required. However, water and ethanol form an atmospheric azeotrope at 96.5% wt, so it is not possible to achieve the desired product by applying only distillation unit. Thus, in this step, a combination of distillation and molecular sieves was employed. Firstly, the broth from the fermentation part was distilled until an ethanol purity of 90% wt. Then, the rest of water was removed using molecular sieves, which is a vapor dehydration process that is based on the adsorption of water molecules on sieve micropores [50].

For the first step of bioethanol recovery, a RadFrac module was selected as a rigorous distillation unit. According to the preliminary shortcut calculations, a total condenser and a kettle reboiler were chosen, and the stage number of the column was set to 25, with the feed entering at stage 11. The design specs featured in Aspen Plus were used to design a column capable of obtaining a product purity of 90% and mole recovery of 99%, minimizing the loss of ethanol in the bottoms. Based on these design specifications, the mass distillate-to-feed and reflux ratios were calculated. Finally, the molecular sieve unit was modeled using a separator block that generated a pure ethanol stream (with a purity of 99%) as the final product of the simulated plant.

3. Results and Discussion

The results from the established simulation model in this paper for the 20 H&AB options, are listed and ranked in Figure 2 according to their share to the specific mass flow rate of bioethanol $sm_{ethanol} = m_{ethanol}$ (g)/$m_{biomass}$ (kg). This ordering was based on the $sm_{ethanol}$ hat was in the range from 99 to 250 g/kg, values highlighting the minimum and the maximum efficient alternatives, respectively. The systems were divided based on their outputs into three classes. Class 1 included six H&AB gasification systems mostly based on straw feedstocks including rice husks, pepper residue, barley straw, walnut hulls and blows, oat straw, and rice straw, which produced the minimum values of $sm_{ethanol}$ (these were in the range of 99–150 g/kg). Seven of the studied H&AB gasification systems were placed in the second class because their output $sm_{ethanol}$ was in the range of 150–200 g per one kg of feedstock. Finally, the third class included seven H&AB options that mainly relied on the shell and grass residues containing sugar cane bagasse, rape straw, sweet sorghum grass, grape marc, bamboo whole, almond shells, and hazelnut shells, which produced relatively higher bioethanol amounts.

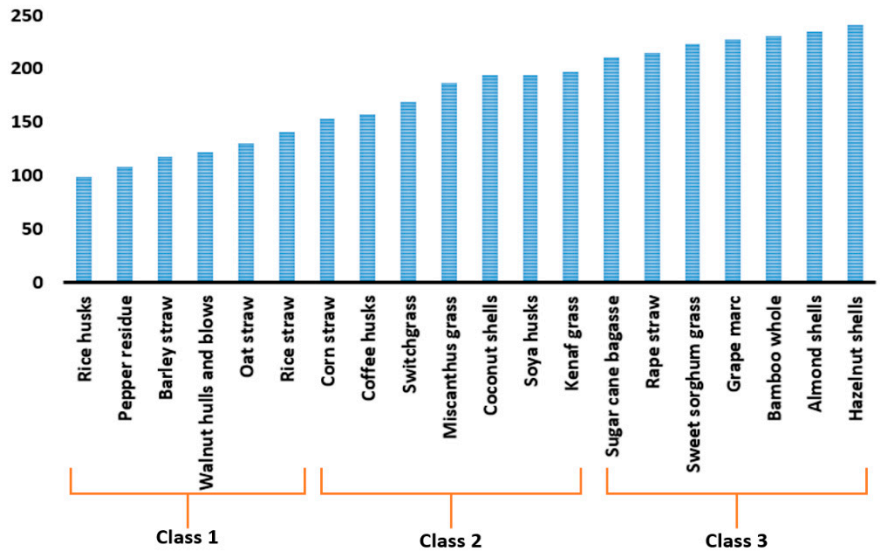

Figure 2. Specific mass flow rate of bioethanol from 20 H&AB gasification systems (gasifier temperature of 900 °C and air-to-fuel ratio of 2).

The system that used hazelnut shell biomass as feedstock remarkably had the highest rank from the viewpoint of bioethanol production (241 g/kg) because of the beneficial results of the performance analysis. This can be explained by the fact that the hazelnut shells had the highest percentage of carbon, hydrogen, and oxygen; very low amounts of ash and nitrogen; and no sulphur (Figure 3). The percentage shares presented in Figure 3 are the contributions of carbon, hydrogen, oxygen, ash, nitrogen, and sulphur in the elemental analysis of each feedstock. Indeed, carbon and hydrogen were found to be essential components in each biomass. Therefore, the greater the C and H_2 contents in the feedstock, the higher carbon monoxide and hydrogen in the syngas product, which

necessarily leads to an amendment of the calorific value of the syngas output. CO and H_2 were found to be the main components in the gas products that were transformed into ethanol and acetic acid (mainly ethanol) in the fermentation reactor. As such, the increase of CO and H_2 in the syngas led to much greater values of ethanol in the output stream.

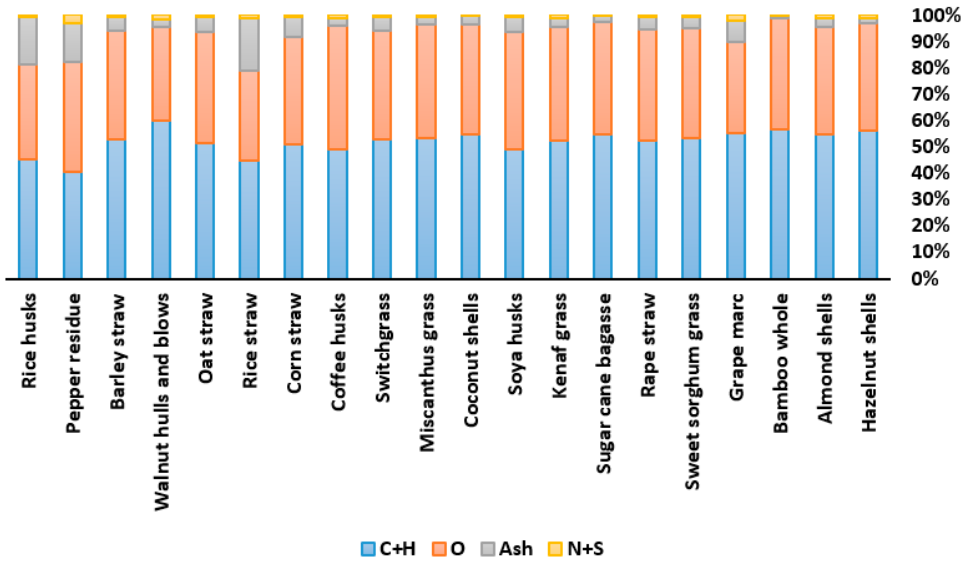

Figure 3. Percentage shares of composition elements for different H&ABs.

Next, the effect of gasifier temperature on the specific mass flow rate of bioethanol obtained from 20 herbaceous and agricultural biomass alternatives is analyzed (Figure 4). The analyses in Figure 4 were carried out at standard conditions of 1 kg of input biomass, an air-to-fuel ratio (AFR) of 2, and varied gasification temperatures in the range of 600–1500 °C. For all evaluated H&ABs, the $sm_{ethanol}$ produced from each plant was modified by addition in the operated temperature. At low temperatures, around 600 °C, the carbon in the biomass material was not consumed/combusted completely, so the syngas product could not reach an appropriate value. Specifically, at lower temperatures, unburned/unused methane and carbon stayed in the output without any change; however, increasing the reactor temperature led to a much greater amount of carbon being partially oxidized and transformed into CO based on the partial combustion reaction. Moreover, the reverse methanation reaction led to methane being converted to H_2. A water–gas reaction also led to the creation of both CO and H_2 at high temperatures. However, increasing the gasification temperature was beneficial for H_2 and CO production, as the yields of H_2 and CO were saturated at high temperatures. The saturation temperature is called the optimum gasifier temperature, which may be different for each system. Bioethanol production also follows this trend because the fermentation part is mainly affected by the syngas input to its process. $sm_{ethanol}$ also increases in a gradual way near the optimum temperature. The optimum operating temperature of the down draft gasifier for H&ABs was found to be in the range of 850–1000 °C.

Variation in the amount of air injected into the system was able to significantly affect the substances and quality of the syngas produced, as well as the bioethanol production. The quantity of air entering the gasification can be expressed as a factor of the AFR, which is the mass flow rate of the required air input to burn a mass unit of dry fuel. The impacts of AFR on the bioethanol obtained via the gasification alternatives fed by 20 H&ABs are depicted in Figure 5. In this analysis, all operating parameters except for AFR were considered constant, with a gasifier temperate of 900 °C and 1 kg of input biomass. The optimum values of AFR for H&AB gasification plants were found to be in the range of 1.8–2.3. In fact, at smaller AFR levels, biomass gasification acted like the pyrolysis process, so charcoal remained and came with energy losses. Nevertheless, at greater AFR levels, the extra supplied oxygen was combusted with carbon and carbon monoxide, which led

to a reduction in high quality syngas production. Therefore, it was critical to find the proper values of AFR for H&AB gasification linked with ethanol production, which was investigated in this work. As shown in Figure 5, the optimum AFR values for the highest specific mass flow rates of H&ABs were found to be between 1.95 and 2 for H&ABs in classes 2 and 3 and between 1.8 and 1.9 for H&ABs located in class 1.

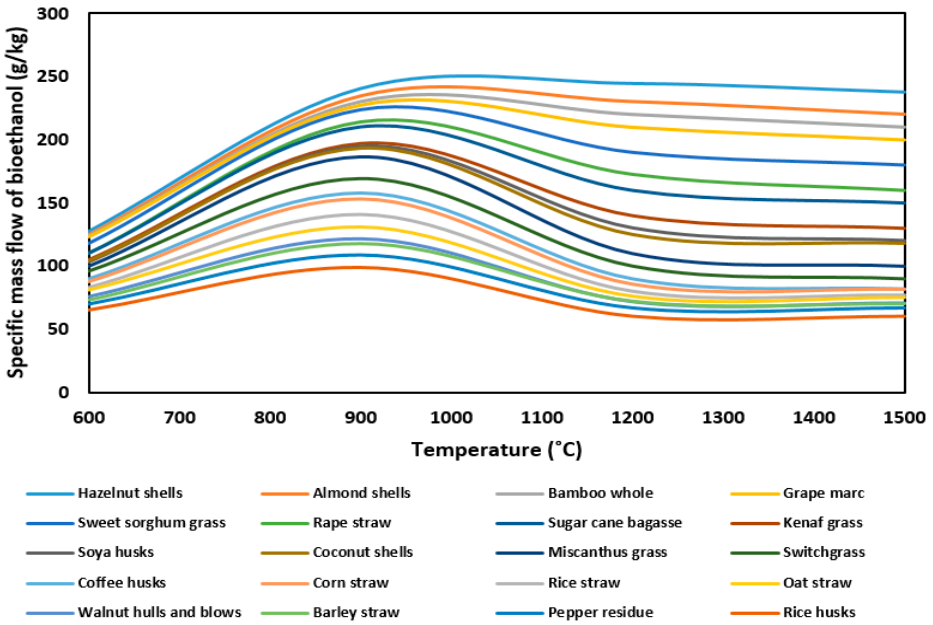

Figure 4. Effect of gasifier temperature on $sm_{ethanol}$ for 20 H&ABs.

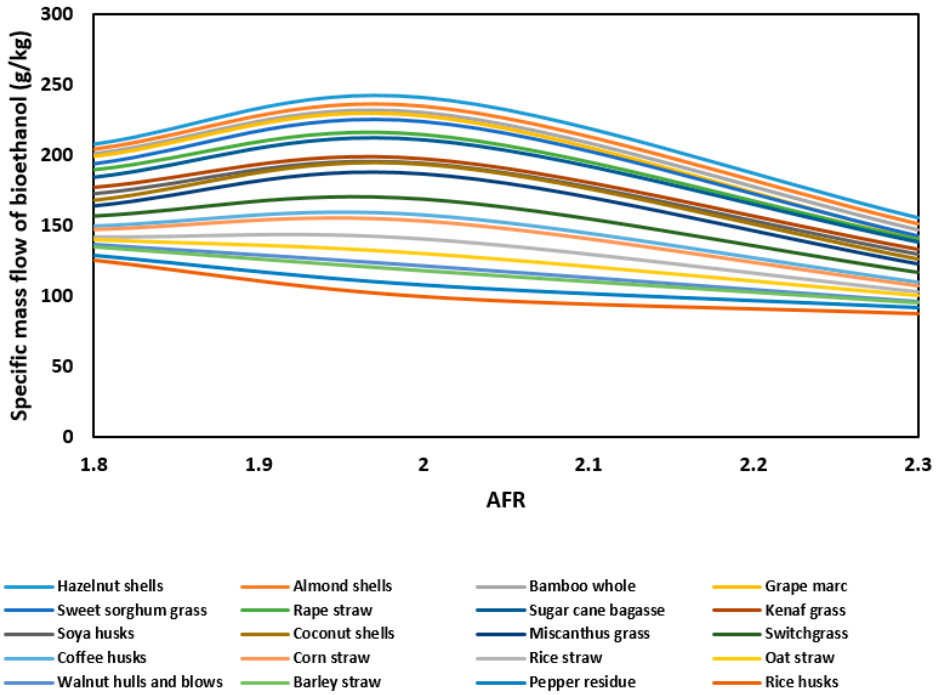

Figure 5. Effect of the air-to-fuel ratio on $sm_{ethanol}$ for 20 H&ABs.

4. Conclusions

In this paper, a biomass gasification simulation model was established based on the non-stoichiometric equilibrium method via ASPEN Plus. The developed model contains the main process/submodules necessary for the method, such as drying, pyrolysis, and gasification linked with the syngas fermentation and product purification units for

bioethanol production. The established model was evaluated for different 20 herbaceous and agricultural biomasses under various operating parameters to find the optimum conditions for the highest bioethanol production.

This model can be used for the prediction of various outputs like values of bioethanol gained from a huge number of biomass feedstocks with defined ultimate compositions and proximate analysis under various operating conditions such as air flow rate and temperature. The presented simulation model is a useful tool for the preliminary calculations, design, and operation of biomass gasifiers. Moreover, this model can be used for the evaluation of several options to allow for decision-makers to create efficient infrastructures in the energy management sector.

The obtained results of the developed simulation model for 20 H&AB alternatives showed that the specific mass flow rate of bioethanol produced from 1 kg of feedstock input to the system is 99–250 g/kg, and the alternative fed by hazelnut shell biomass led to a remarkably higher rate (241 g/kg) than those of other plants, as seen in the beneficial results obtained from the performance analysis. In the model, sensitivity analysis was also performed, and the impact of varying the gasifier temperature and AFR on $sm_{ethanol}$ from each system was investigated. Raising the temperature was found to improve gasifier performance by increasing the creation of CO and H_2, which led to a greater output of bioethanol. Nevertheless, increasing the AFR was found to degrade the CO and H_2 production, which resulted in a reduction in gasification performance.

Author Contributions: S.S.: Conceptualization, Methodology, Simulation, Validation, Formal analysis, Investigation, Resources, Writing of original draft, review & editing. R.U.: Supervision, review & editing. C.R.: Software & Supervision. All authors have read and agreed to the published version of the manuscript.

Funding: This paper was a part of the project funded by Icelandic Research Fund (IRF), (in Icelandic: Rannsoknasjodur), and the grant number is 196458-051.

Institutional Review Board Statement: Not applicable.

Informed Consent Statement: Not applicable.

Data Availability Statement: Not applicable.

Conflicts of Interest: The authors declare no conflict of interest.

References

1. Safarian, S.; Khodaparast, P.; Kateb, M. Modeling and Technical–Economic Optimization of Electricity Supply Network by Three Photovoltaic Systems. *J. Sol. Energy Eng.* **2014**, *136*, 024501. [CrossRef]
2. Safarian, S.; Unnthorsson, R.; Richter, C. Techno–Economic Analysis of Power Production by Using Waste Biomass Gasification. *J. Power Energy Eng.* **2020**, *8*, 1. [CrossRef]
3. Begum, S.; Rasul, M.; Akbar, D.A. Numerical Investigation of Municipal Solid Waste Gasification Using Aspen Plus. *Procedia Eng.* **2014**, *90*, 710–717. [CrossRef]
4. Zeng, J.; Xiao, R.; Zhang, H.; Wang, Y.; Zeng, D.; Ma, Z. Chemical Looping Pyrolysis–Gasification of Biomass for High H2/CO Syngas Production. *Fuel Process. Technol.* **2017**, *168*, 116–122. [CrossRef]
5. Luo, H.; Lin, W.; Song, W.; Li, S.; Dam-Johansen, K.; Wu, H. Three Dimensional Full–Loop CFD Simulation of Hydrodynamics in a Pilot–Scale Dual Fluidized Bed System for Biomass Gasification. *Fuel Process. Technol.* **2019**, *195*, 106146. [CrossRef]
6. Kumar, B.; Bhardwaj, N.; Agrawal, K.; Chaturvedi, V.; Verma, P. Current Perspective on Pretreatment Technologies using Lignocellulosic Biomass: An Emerging Biorefinery Concept. *Fuel Process. Technol.* **2020**, *199*, 106244. [CrossRef]
7. Safarian, S.; Unnthorsson, R.; Richter, C. Hydrogen Production via Biomass Gasification: Simulation and Performance Analysis under Different Gasifying Agents. *Biofuels* **2021**, 1–10. [CrossRef]
8. Amaducci, S.; Facciotto, G.; Bergante, S.; Perego, A.; Serra, P.; Ferrarini, A.; Chimento, C. Biomass Production and Energy Balance of Herbaceous and Woody Crops on Marginal Soils in the Po Valley. *Gcb Bioenergy* **2017**, *9*, 31–45. [CrossRef]
9. Shankar Tumuluru, J.; Sokhansanj, S.; Hess, J.R.; Wright, C.T.; Boardman, R.D. A Review on Biomass Torrefaction Process and Product Properties for Energy Applications. *Ind. Biotechnol.* **2011**, *7*, 384–401. [CrossRef]
10. Talebnia, F.; Karakashev, D.; Angelidaki, I. Production of Bioethanol from Wheat Straw: An Overview on Pretreatment, Hydrolysis and Fermentation. *Bioresour. Technol.* **2010**, *101*, 4744–4753. [CrossRef]
11. Safarian, S.; Sattari, S.; Unnthorsson, R.; Hamidzadeh, Z. Prioritization of Bioethanol Production Systems from Agricultural and Waste Agricultural Biomass Using Multi–criteria Decision Making. *Biophys. Econ. Resour. Qual.* **2019**, *4*, 4. [CrossRef]

12. Safarian, S.; Unnthorsson, R. An Assessment of The Sustainability of Lignocellulosic Bioethanol Production from Wastes in Iceland. *Energies* **2018**, *11*, 1493. [CrossRef]
13. Hirschnitz-Garbers, M.; Gosens, J. Producing Bio–Ethanol from Residues and Wastes: A Technology with Enormous Potential in need of Further Research and Development. *Policy Brief* **2015**, *5*, 1–5.
14. Michailos, S.; Parker, D.; Webb, C. Design, Sustainability Analysis and Multiobjective Optimisation of Ethanol Production via Syngas Fermentation. *Waste Biomass Valorization* **2017**, *10*, 1–12. [CrossRef]
15. Liguori, R.; Soccol, C.R.; Porto de Souza Vandenberghe, L.; Woiciechowski, A.L.; Faraco, V. Second Generation Ethanol Production from Brewers' Spent Grain. *Energies* **2015**, *8*, 2575–2586. [CrossRef]
16. Mu, D.; Seager, T.; Rao, P.S.; Zhao, F. Comparative Life Cycle Assessment of Lignocellulosic Ethanol Production: Biochemical Versus Thermochemical Conversion. *Environ. Manag.* **2010**, *46*, 565–578. [CrossRef]
17. Safarian, S.; Unnthorsson, R.; Richter, C. Simulation and Performance Analysis of Integrated Gasification–Syngas Fermentation Plant for Lignocellulosic Ethanol Production. *Fermentation* **2020**, *6*, 68. [CrossRef]
18. Pardo-Planas, O.; Atiyeh, H.K.; Phillips, J.R.; Aichele, C.P.; Mohammad, S. Process. Simulation of Ethanol Production from Biomass Gasification and Syngas Fermentation. *Bioresour. Technol.* **2017**, *245*, 925–932. [CrossRef] [PubMed]
19. Safarian, S.; Unnthorsson, R.; Richter, C. Techno–Economic and Environmental Assessment of Power Supply Chain by using Waste Biomass Gasification in Iceland. *Biophys. Econ. Sustain.* **2020**, *5*, 7. [CrossRef]
20. Safarian, S.; Ebrahimi Saryazdi, S.M.; Unnthorsson, R.; Richter, C. Gasification of Woody Biomasses and Forestry Residues: Simulation, Performance Analysis, and Environmental Impact. *Fermentation* **2021**, *7*, 61. [CrossRef]
21. Phillips, J.R.; Huhnke, R.L.; Atiyeh, H.K. Syngas Fermentation: A Microbial Conversion Process of Gaseous Substrates to Various Products. *Fermentation* **2017**, *3*, 28. [CrossRef]
22. de Medeiros, E.M.; Posada, J.A.; Noorman, H.; Filho, R.M. Dynamic Modeling of Syngas Fermentation in a Continuous Stirred–Tank Reactor: Multi–response Parameter Estimation and Process Optimization. *Biotechnol. Bioeng.* **2019**, *116*, 2473–2487. [CrossRef]
23. Munasinghe, P.C.; Khanal, S.K. Biomass–Derived Syngas Fermentation into Biofuels: Opportunities and Challenges. *Bioresour. Technol.* **2010**, *101*, 5013–5022. [CrossRef]
24. Sun, X.; Atiyeh, H.K.; Huhnke, R.L.; Tanner, R.S. Syngas Fermentation Process Development for Production of Biofuels and Chemicals: A Review. *Bioresour. Technol. Rep.* **2019**, *7*, 100279. [CrossRef]
25. Safarian, S.; Unnthorsson, R.; Richter, C. Performance Analysis of Power Generation by Wood and Woody Biomass Gasification in a Downdraft Gasifier. *J. Appl. Power Eng.* **2021**, *10*, 80–88.
26. Safarianbana, S.; Unnthorsson, R.; Richter, C. Development of A New Stoichiometric Equilibrium–based Model for Wood Chips and Mixed Paper Wastes Gasification by ASPEN Plus. In Proceedings of the ASME International Mechanical Engineering Congress and Exposition, Portland, OR, USA, 11 November 2019.
27. Safarian, S.; Unnthorsson, R.; Richter, C. Performance Analysis and Environmental Assessment of Small–Scale Waste Biomass Gasification Integrated CHP in Iceland. *Energy* **2020**, *197*, 117268. [CrossRef]
28. Safarian, S.; Unnthorsson, R.; Richter, C. Simulation of Small–Scale Waste Biomass Gasification Integrated Power Production: A Comparative Performance Analysis for Timber and Wood Waste. *Int. J. Appl. Power Eng.* **2020**, *9*, 147–152. [CrossRef]
29. Vassilev, S.V.; Baxter, D.; Andersen, L.K.; Vassileva, C.G. An Overview of The Chemical Composition of Biomass. *Fuel* **2010**, *89*, 913–933. [CrossRef]
30. Demirbas, A. Combustion characteristics of different biomass fuels. *Prog. Energy Combust. Sci.* **2004**, *30*, 219–230. [CrossRef]
31. Scurlock, J.M.; Dayton, D.C.; Hames, B. Bamboo: An Overlooked Biomass Resource? *Biomass Bioenergy* **2000**, *19*, 229–244. [CrossRef]
32. Risnes, H.; Fjellerup, J.; Henriksen, U.; Moilanen, A.; Norby, P.; Papadakis, K.; Posselt, D.; Sørensen, L. Calcium Addition in Straw Gasification. *Fuel* **2003**, *82*, 641–651. [CrossRef]
33. Thy, P.; Lesher, C.; Jenkins, B. Experimental Determination of High–Temperature Elemental Losses from Biomass Slag. *Fuel* **2000**, *79*, 693–700. [CrossRef]
34. Moilanen, A. Thermogravimetric Characterisations of Biomass and Waste for Gasification Processes. *VTT* **2006**, *607*, 1–103.
35. Theis, M.; Skrifvars, B.-J.; Hupa, M.; Tran, H. Fouling Tendency of Ash Resulting from Burning Mixtures of Biofuels. Part. 1: Deposition Rates. *Fuel* **2006**, *85*, 1125–1130. [CrossRef]
36. Thy, P.; Jenkins, B.; Grundvig, S.; Shiraki, R.; Lesher, C. High. Temperature Elemental Losses and Mineralogical Changes in Common Biomass Ashes. *Fuel* **2006**, *85*, 783–795. [CrossRef]
37. Werther, J.; Saenger, M.; Hartge, E.-U.; Ogada, T.; Siagi, Z. Combustion of Agricultural Residues. *Prog. Energy Combust. Sci.* **2000**, *26*, 1–27. [CrossRef]
38. Miles, T.; Baxter, L.; Bryers, R.; Jenkins, B.; Oden, L. Alkali Deposits Found in Biomass Power Plants: A Preliminary Investigation of Their Extent and Nature. *Alikali Depos. Found Biomass Power Plants* **1995**. [CrossRef]
39. Masiá, A.T.; Buhre, B.; Gupta, R.; Wall, T. Characterising Ash of Biomass and Waste. *Fuel Process. Technol.* **2007**, *88*, 1071–1081. [CrossRef]
40. Nutalapati, D.; Gupta, R.; Moghtaderi, B.; Wall, T. Assessing Slagging and Fouling During Biomass Combustion: A Thermodynamic Approach Allowing for Alkali/Ash Reactions. *Fuel Process. Technol.* **2007**, *88*, 1044–1052. [CrossRef]

41. Safarian, S.; Ebrahimi Saryazdi, S.M.; Unnthorsson, R.; Richter, C. Artificial Neural Network Modeling of Bioethanol Production Via Syngas Fermentation. *Biophys. Econ. Sustain.* **2021**, *6*, 1. [CrossRef]
42. Safarian, S.; Ebrahimi Saryazdi, S.M.; Unnthorsson, R.; Richter, C. Dataset of Biomass Characteristics and Net Output Power from Downdraft Biomass Gasifier Integrated Power Production Unit. *Data Brief* **2020**, *33*, 106390. [CrossRef]
43. Safarian, S.; Ebrahimi Saryazdi, S.M.; Unnthorsson, R.; Richter, C. Modeling of Hydrogen Production by Applying Biomass Gasification: Artificial Neural Network Modeling Approach. *Fermentation* **2021**, *7*, 71. [CrossRef]
44. Safarian, S.; Ebrahimi Saryazdi, S.M.; Unnthorsson, R.; Richter, C. Artificial Neural Network Integrated with Thermodynamic Equilibrium Modeling of Downdraft Biomass Gasification–Power Production Plant. *Energy* **2020**, *213*, 118800. [CrossRef]
45. Damartzis, T.; Michailos, S.; Zabaniotou, A. Energetic Assessment of a Combined Heat and Power Integrated Biomass Gasification–Internal Combustion Engine System by using Aspen Plus®. *Fuel Process. Technol.* **2012**, *95*, 37–44. [CrossRef]
46. Tauqir, W.; Zubair, M.; Nazir, H. Parametric Analysis of a Steady State Equilibrium–Based Biomass Gasification Model for Syngas and Biochar Production and Heat Generation. *Energy Convers. Manag.* **2019**, *199*, 111954. [CrossRef]
47. Safarian, S.; Unnthorsson, R.; Richter, C. The Equivalence of Stoichiometric and Non–Stoichiometric Methods for Modeling Gasification and Other Reaction Equilibria. *Renew. Sustain. Energy Rev.* **2020**, *131*, 109982. [CrossRef]
48. Safarianbana, S. Simulation of a Small Scale Biowaste Gasification System for Energy Production. PhD Dissertation, University of Iceland, Reykjavík, Iceland, 2021.
49. Ray, R.C.; Ramachandran, S. *Bioethanol Production from Food Crops: Sustainable Sources, Interventions, and Challenges*; Academic Press: Cambridge, MA, USA, 2018.
50. Teo, W.K.; Ruthven, D.M. Adsorption of Water from Aqueous Ethanol using 3–. ANG. Molecular Sieves. *Ind. Eng. Chem. Process. Des. Dev.* **1986**, *25*, 17–21. [CrossRef]